THE JOURNAL OF PHYSICAL CHEMISTRY B

ARTICLE

pubs.acs.org/JPCB

# $^{15}$N Solid-State NMR as a Probe of Flavin H-Bonding

Dongtao Cui,[†,¶] Ronald L. Koder, Jr.,[‡,#] P. Leslie Dutton,[‡] and Anne-Frances Miller*[,†]

[†]Department of Chemistry, University of Kentucky, Lexington, Kentucky 40506-0055, United States

[‡]The Johnson Foundation and Department Biochemistry, University of Pennsylvania, Philadelphia, Pennsylvania 19104-6059, United States

Supporting Information

**ABSTRACT:** Flavins mediate a wide variety of chemical reactions in biology. To learn how one cofactor can be made to execute different reactions in different enzymes, we are developing solid-state NMR (SSNMR) to probe the flavin electronic structure, via the $^{15}$N chemical shift tensor principal values ($\delta_{ii}$). We find that SSNMR has superior responsiveness to H-bonds, compared to solution NMR. H-bonding to a model of the flavodoxin active site produced an *in*crease of 10 ppm in the $\delta_{11}$ of N5, although none of the H-bonds directly engage N5, and solution NMR detected only a 4 ppm increase in the isotropic chemical shift ($\delta_{iso}$). Moreover SSNMR responded differently to different H-bonding environments, as H-bonding with water caused $\delta_{11}$ to *de*crease by 6 ppm, whereas $\delta_{iso}$ increased by less than 1 ppm. Our density functional theoretical (DFT) calculations reproduce the observations, validating the use of computed electronic structures to understand *how* H-bonds modulate the flavin's reactivity.

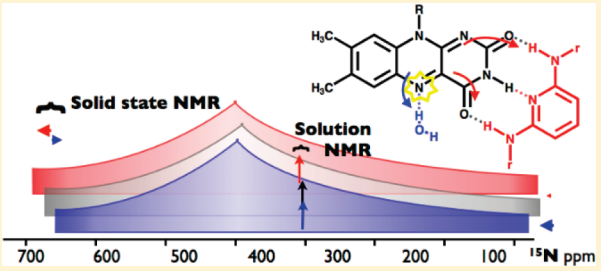


## 1. INTRODUCTION

Flavoenzymes, containing flavin adenine dinucleotide (FAD)[1] or flavin mononucleotide (FMN) as a prosthetic group, catalyze an enormous variety of reactions, including dehydrogenation, monooxygenation, disulfide reduction, signaling, DNA repair, magnetic sensing, chemiluminescence, and more.[2,3] The use of such chemically versatile cofactors provides metabolic economy in that relatively few different cofactors are needed for life, but produces the requirement that individual enzymes be able to restrict their bound cofactor's reactivity to a fraction of its innate repertoire. This problem is thus fairly general and can be expected to also occur in enzymes that employ other versatile cofactors, such as pterins, pyridoxal/amine phosphate, and biotin.

Massey and Hemmerich proposed that different flavoenzymes could achieve their distinct reactivities by favoring different resonance structures of their bound flavins.[4] Our modern rephrasing of this idea is to propose that different reactivities will be associated with different tuning of the natures and relative energies of the frontier orbitals. In most cases this must be accomplished via noncovalent interactions between the cofactor and the protein that vary from enzyme to enzyme. Interactions commonly observed to modulate flavin reactivity include steric distortion of the ring system,[5−7] placement of local charges,[8,9] stacking with aromatic side chains,[10,11] modulation of the pKs of redox-coupled protons,[12] local polarity,[13] and, importantly, H-bonding.[3,14−16] As a step toward eventually understanding how proteins modulate flavin reactivity, we are developing a methodology for observing and assessing the effects of H-bonding on the flavin's electronic structure.

Flavin electronic structure has been studied by numerous methods including absorption spectrophotometry,[9,17] luminescence,[18] circular dichroism,[19] and Stark spectroscopy[20,21] to characterize the local environment and interactions between the flavin and nearby functional groups. Vibrational spectroscopy of several sorts has been used to report on more localized interactions and effects of binding to the protein.[22,23] NMR spectroscopy provides the ultimate spatial resolution via its detection of signals from individual atoms. Solution-state NMR has been used extensively to infer bond order, the existence and strength of H-bonding, and more.[14,24−26] Indeed, the isotropic chemical shifts ($\delta_{iso}$s)[1] measured in solution for individual flavin ring C and N atoms vary by over more than 10 and 40 ppm, respectively, among flavins in different environments.[24]

Solid-state NMR (SSNMR) measurements have the additional advantage that all three chemical shift tensor principal values[27] (CSPVs, $\delta_{11}$, $\delta_{22}$, and $\delta_{33}$) can be measured for each atom.[28] Hence, SSNMR can detect chemical shift changes that affect different principal values in opposite directions and thus cancel out the isotropic average ($\delta_{iso} = (\delta_{11} + \delta_{22} + \delta_{33})/3$). Moreover, the flavin N atoms N1 and N5 of the redox-active diazabutadiene core (Scheme 1) both constitute uniquely favorable cases for characterization by SSNMR, as the $\delta_{11}$ of such 6-n[29] pyridine-type[24] sites has been shown to be very sensitive to interactions affecting the nonbonded lone pair,[30] consistent with Ramsey's equation[31] and studies of simpler heterocycles by Grant, Wasylishen, and Oldfield.[29,32,33] At a fundamental level,

**Received:** March 6, 2011
**Revised:** May 6, 2011
**Published:** May 27, 2011

**Scheme 1. Structure of TPARF (Black) in Complex with DBAP (Gray), Showing the Numbering of the Flavin N Positions**[a]

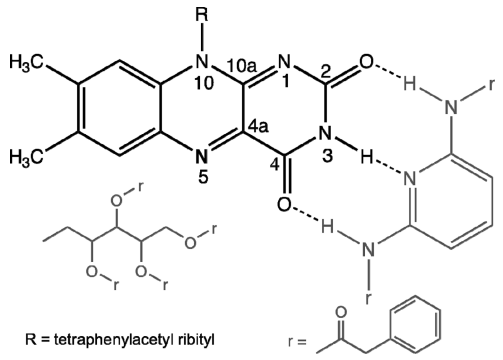


[a] The flavin variants discussed herein are distinguished only by their side chains: R = methyl for lumiflavin (LF); R = ribitylphosphate for FMN; R = ribityladenosine diphosphate for FAD, R = tetraacetylribityl for TARF, and R = tetraphenylacetylribityl for TPARF.

the paramagnetic contribution to the chemical shift reflects the extent to which high-lying occupied orbitals (HOMOs)[34] and low-lying excited-state orbitals (LUMOs) can be mixed by orbital angular momentum. This is relatively large in aromatic systems where the separation between the LUMO and the HOMO is relatively small. Moreover, because the HOMOs and LUMOs are also the orbitals that play the largest role in reactivity, the CSPVs are expected to be related to reactivity and its modulation by proteins. Thus, not only does SSNMR yield three times more descriptors of each atom than solution NMR but also the CSPVs of oxidized flavins may be related to the very orbitals that are expected to dominate the chemistry.

SSNMR of $^{15}$N has been established as a method of probing the structure of the peptide backbone[35−37] as well as H-bonding of amino acid side chains.[38,39] It promises to be equally applicable to the organic cofactors and transition states that are central to the reactivity of many enzymes.[40] Indeed, $^{15}$N and $^{13}$C isotropic chemical shifts of an intermediate in tryptophan synthase were used to determine the protonation states of reacting groups,[41] and Paramasivam et al. have shown that $^{13}$C and $^{15}$N chemical shifts as well as chemical shift anisotropies are sensitive reporters of the protonation state and tautomerization of thiamine.[42] Likewise, previous SSNMR studies of a model flavin demonstrated that very different CSPVs clearly differentiate between the N5 and N1 sites, consistent with N5 and N1's distinct electronic properties and reactivities.[30,43]

In our effort to understand the effects of H-bonds on flavin electronic structure, we sought to compare the NMR signatures produced by two different H-bonding environments. Such studies in the past have compared flavin alone with flavin in a complex and found that the reduction midpoint potential could be shifted by some 100−150 mV upon H-bonding to a synthetic model of the active site of lipoamide dehydrogenase and flavodoxin.[44] However, it is clear that the commonly used solvent $CHCl_3$ significantly attenuated the effect of added H-bonding partners,[45] and recent work shows that this solvent interacts with the flavin, acting as a H-bond donor itself.[46] Thus, many studies likely document the effect of displacement of solvent by the H-bonding partner. To be able to work in a non-H-bonding solvent, we designed and synthesized a new flavin model, tetraphenylacetylriboflavin (TPARF), wherein the ribityl side chain is decorated with four benzyl groups that dissolve readily in benzene.[47] As a result, TPARF is soluble in benzene to over 250 mM, and electrochemical analysis of TPARF both alone and in complexes with benzene-soluble H-bonding partners demonstrated that this system behaves similarly to other flavin model systems.[44,46] The hope was that this system could minimize the effect of solvent on the results of our measurements.

We have used TPARF and its complex with a benzene-soluble H-bonding partner dibenzylamidopyridine (DBAP, Scheme 1), inspired by earlier work by Yano and Rotello on diamidopyridine.[44,48] DBAP binds to TPARF with a $K_d$ of 420 $\mu$M in benzene and raises the flavin's oxidized/semiquinone reduction potential by 100 mV.[46] Thus, the DBAP complex provides us with a stable benzene-soluble model wherein H-bond formation modulates the reactivity of a flavin.

Given our goal of understanding how different interactions can modulate flavin reactivity, we begin by focusing on the N5 site of the flavin ring (Scheme 1), as this is one of the two redox-active N's and the site of hydride acceptance.[3] The chemical shift tensor of N5 is over 700 ppm wide.[30] This is consistent with Ramsey's equation, our earlier calculations, and prior work on simpler pyridine-like systems.[29,31] Thus, interactions that modulate the energy of the $\pi^*$ or n orbitals are observed to have strong effects on $\delta_{11}$.[29,38] To focus on N5, we have synthesized TPARF incorporating $^{15}$N at that position only and now describe the responses of N5′s CSPVs to formation of a well-defined H-bonded complex with DBAP vs the effects H-bonding in less well-defined interactions with water or in flavin dimers. Our spectroscopic measurements and calculations demonstrate that $^{15}$N CSPVs are sensitive and informative tools for revealing the existence of H-bonding interactions and for distinguishing among different patterns of H-bonding. Thus, we anticipate that $^{15}$N-SSNMR in conjunction with DFT calculations will be a valuable complement to other methods for understanding the effects of noncovalent interactions such as those used by proteins to modulate flavin reactivity. A better understanding of the electronic structures of these cofactors would greatly improve our understanding of catalytic mechanisms and our ability to manipulate or build upon them.

## 2. EXPERIMENTAL METHODS

**2.1. Synthesis.** [$^{15}$N-N5] TPARF and DBAP were synthesized according to published methods.[46,47] All the benzene used was DriSolv benzene, purchased from EMD, and maintained under argon.

**2.2. Optical Spectra.** Solid TPARF and DBAP were each dissolved in benzene. All optical spectra were obtained using a HP-8452B diode array spectrophotometer. Concentrated solutions were studied in a 1 mm path length cell, to ensure that all absorbance readings were below 0.8.

**2.3. Solution NMR.** TPARF or TPARF + DBAP were dissolved in deuterated benzene from a fresh ampule (Cambridge Isotopes) to final concentrations of up to 7 mM TPARF and saturating DBAP. Water was added to a concentration five times that of TPARF. Data were collected at 25 °C on a 600 MHz Varian Inova spectrometer at 60 MHz for $^{15}$N using an automatic switchable broad-band probe. Spectra employed a 45° excitation pulse followed by 0.25 s of data acquisition and then a 4 s delay for relaxation. The chemical shift was referenced to external $^{15}$N urea in DMSO at 25 °C.

**2.4. Solid-State NMR Conditions.** All data were collected at a nominal temperature of −60 °C (see Supporting Information).

The low temperature was found to increase the $^{15}N$ signal-to-noise while also maintaining benzene in its solid state (freezing point = 5.5 °C). Solid TPARF (0.124 g = 0.146 mmol) was packed in a 5 mm zirconia rotor. Samples composed of 80 $\mu$L of 200 mM TPARF in benzene, 80 $\mu$L of 200 mM TPARF in benzene with saturating DBAP (undissolved excess was visible as a small amount of white powder that settled in the bottom of the tube and was allowed to remain in the sample), or 80 $\mu$L of 200 mM TPARF in benzene with 1.6 $\mu$L of $H_2O$ were each contained in delrin vials custom machined to fit snugly into our 5 mm zirconia rotors. 1.6 $\mu$L of water provides five stoichiometric equivalents of water per flavin and exceeds the solubility of water in benzene. A sample containing three times as much water was also characterized and found to produce the same CSPVs as the 1.6 $\mu$L-containing sample. Attempts to identify benzene:toluene mixtures that would freeze as glasses were unsuccessful, and TPARF is insoluble in cyclohexane. Rotors were frozen vertically in dry ice/acetone, loaded into the probe at 0 °C, and then cooled to −60 °C while spinning at the magic angle at 5 kHz.

$^{15}N$ magic angle spinning (MAS) spectra were collected at 40 MHz for $^{15}N$ with signal enhancement via ramped cross-polarization (CP) from $^{1}H$ in 5 mm Zr rotors in an HX Chemagnetics-type probe using a Varian Inova spectrometer. $^{15}N$ spectra were collected with interscan delays of 5 s, CP contact times of 8 ms at a CP field of 50 kHz for $^{1}H$, and $^{1}H$ TPPM2 decoupling at 50 kHz during the 20 ms acquisitions.[49] Spinning speeds of 3000, 4000, and 5000 Hz were used for the $^{15}N$ 1-dimensional CP-MAS spectra used to determine $^{15}N$ CSPVs (Supporting Information, Table S1). All $^{15}N$ chemical shifts are quoted relative to liquid ammonia, and spectra were referenced indirectly based on the $^{15}NH_4^+$ signals of $NH_4NO_3$ at 21 ppm.[50]

The intensity distribution among the spinning side bands yielded the three CSPVs of the signal via Herzfeld−Berger analysis for each spectrum.[51,52] Averages of the values obtained at MAS speeds of 3000, 4000, and 5000 Hz weighted each set of CSPVs according to the chi-squared value associated with its Herzfeld−Berger fit. Reported standard deviations thus reflect the quality of the Herzfeld−Berger fits in addition to the experimental scatter. Experimental uncertainties associated with the reported CSPVs were determined to be 1−2 ppm based on the reproducibility of the values obtained from replicate experiments conducted months apart on replicate samples (the corresponding uncertainty in the $\delta_{iso}$ was 0.3 ppm).

**2.5. Calculations.** All DFT calculations were performed with the Gaussian 03 package,[53] implemented on the University of Kentucky's N- and X-class HP supercomputers. LF (lumiflavin, see Scheme 1) was used to model the flavin ring system; LF has a methyl group at the N10 position instead of the functionalized ribityl side chain of TPARF, however it retains characteristic flavin reactivity.[54]

Initially, geometry optimizations of oxidized LF and DBAP and the complex between LF and DBAP were done with each of B3PW91[55] and B3LYP[56] and a range of different basis sets. Plots of the LF or LF·DBAP complex energy versus the number of basis functions used in the optimization provided estimates of the point of saturation of the basis sets (Supporting Information, Figure 1S).

Basis sets deemed to have reached the point of diminishing returns were tested for their ability to reproduce experimental CSPVs. NMR chemical shift calculations employed the gauge including atomic orbital (GIAO) method[57] for both B3PW91 and B3LYP with 6-311++G(d,p), 6-311G(2d,2p), 6-311+G(2d,2p), and 6-311++G(2d,2p) basis sets. For each basis, each of the two functionals was used for geometry optimization. Then, each resulting structure was used as the basis for NMR shielding calculation with each of the two functionals, yielding a total of four shielding values for each basis (Supporting Information, Figure 2S). Use of the B3PW91 functional with the 6-311++G-(2d,2p) basis set for both geometry optimization and GIAO chemical shifts calculations best reproduced the experimental $\delta_{iso}$ of N5 in benzene of 346.1 ppm. Similarly, B3PW91 with 6-311++G(2d,2p) yielded a calculated shielding of 261.54 ppm for $NH_3$, very close to the value of 264.54 ppm obtained from spin rotation constants.[59] Thus, our calculations do a very good job of replicating gas-phase measurements. Reported calculations therefore employed B3PW91 and 6-311++G-(2d,2p) with a SCRF (self-consistent reaction field) to account for the effect of benzene's dielectric on the flavin via the polarizable continuum model (PCM).[58] Calculated $^{15}N$ shieldings were converted to calculated chemical shifts by subtracting the former from the shielding of liquid ammonia of 244.6 ppm.[59] Coordinates of geometry-optimized LF and LF·DBAP are included in the Supporting Information (Tables 2S and 3S).

The energies of H-bonds between LF and DBAP were calculated from the energy of the complex minus the energies of the participants, upon counterpoise correction for the basis set superposition error.[60−62] NPA (natural population analysis) charges were used to calculate the distribution of electron density in optimized geometries.[63]

Molecular dynamics calculations (MD) of lumiflavin were executed in HyperChem 8.0, allowing a 2 ns equilibration at a temperature of 213 K with the MM+ force field (Supporting Information, Figure 3S). Ten frames from 1 ps of equilibrated molecular dynamics were used as input for GIAO chemical shielding calculations in Gaussian. These frames included the structure representing the global energy minimum of the MD trajectory as well as the structure representing the following peak energy of the residual energy oscillation (see Supporting Information, Figure 4S). The standard deviations of the obtained CSPVs serve as our estimates of the uncertainties associated with NMR chemical shift calculations stemming from possible deviations between the ideal structure and the real structure. Similarly, we estimated the uncertainty associated with NPA charges based on deviations between those calculated based on different structures from the equilibrated MD.

## 3. RESULTS

**3.1. TPARF in Benzene.** The objective of the current work is to compare the spectral signatures and underlying electronic structures of TPARF alone and in complex with two different H-bonding partners. While prior work establishes that TPARF will form H-bonds with added DBAP or $H_2O$,[46,64] it is not a given that TPARF alone will lack H-bonds. Although we have gone to the trouble of synthesizing a new derivative of flavin to permit its study in noninteracting solvent,[46] one component of the solution that cannot be eliminated is the flavin itself, and two flavin molecules may interact with one another and form dimers. The traditional solution to this problem would be to repeat the experiment at a series of flavin concentrations and extrapolate the results to infinite dilution. Unfortunately, the relative insensitivity of $^{15}N$ NMR requires that flavin concentrations of 1 mM and higher be used. For $^{15}N$ SSNMR, where the signal intensity of N5 is distributed over more than 700 ppm, flavin

**Table 1. Experimental and Calculated $^{15}$N CSPVs[a] of [$^{15}$N-N5] TPARF in Benzene, [$^{15}$N-N5] TPARF in Benzene with DBAP, and [$^{15}$N-N5] TPARF in Benzene with $H_2O$**

| sample | source | $\delta_{11}$ (ppm) | $\delta_{22}$ (ppm) | $\delta_{33}$ (ppm) | $\delta_{iso}$[b] (ppm) |
|---|---|---|---|---|---|
| TPARF dry | exptl[c] | 675 ± 6 | 388 ± 4 | −34 ± 6 | 342.8[d] |
| TPARF in benzene[f] | exptl[c] | 676 ± 3 | 390 ± 2 | −40 ± 6 | 342.0 ± 0.3 |
| | calcd[e,f] | 722 | 398 | −33 | 362 |
| TPARF in benzene with DBAP | exptl[c] | 687 ± 4 | 395 ± 4 | −36 ± 5 | 348.7 ± 0.8 |
| | calcd[e] | 734 | 401 | −33 | 367[e] |
| TPARF in benzene with $H_2O$ | exptl[c] | 670 ± 3 | 391 ± 4 | −34 ± 5 | 342.5 ± 0.3 |
| | calcd[e,g] | 717 | 398 | −33 | 361 |

[a] Chemical shifts are relative to liquid ammonia. [b] $\delta_{iso} = (\delta_{11} + \delta_{22} + \delta_{33})/3$. [c] Experimental values are all averages of three values obtained at three different MAS speeds. Averages weighted each set of CSPVs according to the chi-squared value associated with its Herzfeld−Berger fit. Thus, the standard deviations incorporate both experimental variations in peak intensities as well as variance in the fits, since they are the standard deviations of the set of $\delta$ values obtained from separate data sets each fit independently. [d] Precision limited only by instrumental error, estimated at 0.3 ppm (see Supporting Information Table 1S). [e] All calculations employed B3PW91 with the 6-311++G(2d,2p) basis set. Uncertainties associated with calculated CSPVs are estimated at 5, 1, and 0.7 ppm for $\delta_{11}$, $\delta_{22}$, and $\delta_{33}$, respectively, and that associated with $\delta_{iso}$ is estimated at 2 ppm (see Experimental Section and Supporting Information Figures 3S and 4S). [f] LF in benzene is considered to be a dimer, as per the text. The chemical shifts quoted are Boltzmann-weighted averages of those obtained for the three energetically viable dimers (see text and Supporting Information including Table 4S and Figure 7S). [g] The calculation took into account weak transient binding of water by Boltzmann weighting the effects of water binding at each position on LF; see text and Supporting Information including Figures 11S and 13S for details.

concentrations at least ten times higher are required. Moreover, the fact that we have succeeded in dissolving our flavin in a genuinely non-H-bonding solvent means that the H-bonding functionalities of the flavin are not satisfied by the solvent and therefore more prone to interaction with those of another flavin, than would be the case in a H-bonding solvent. Thus, an inescapable consequence of the use of $^{15}$N NMR and a non-H-bonding solvent is heightened susceptibility to flavin−flavin H-bonds.[65] We therefore begin by assessing the significance of such events via the flavin's solution NMR and optical signals. We also account for their contribution to the measured results via DFT calculations.

The absorbance of TPARF varies linearly with concentration over the range of 0.03 mM to 0.56 mM. However the structure of the signal appears more pronounced at higher concentrations (Supporting Information, Figure 5S). This is consistent with the increase in the prominence of the structure observed upon addition of DBAP to TPARF[46] and suggests that TPARF forms H-bonds at higher concentrations. Prior work indicated that when TPARF engages in H-bonding with DBAP it experiences a 2 nm red-shift in $\lambda_{max}$ from 445 to 447 nm.[46] We observe an analogous small but consistent shift in $\lambda_{max}$ from 445 to 446 nm, between 0.12 and 0.24 mM TPARF, suggesting formation of H-bonds in that concentration range. Thus, although earlier work found that the cyclic voltammetry TPARF was not concentration dependent,[46] that work was restricted to more moderate concentrations of TPARF (≈0.07 mM), and our current data suggest that at the higher concentrations needed for SSNMR the flavins of TPARF may interact.

To assess the significance of possible TPARF dimerization to the NMR studies, we measured the isotropic chemical shift $\delta_{iso}$ by solution NMR, as a function of dilution (Supporting Information, Figure 6S). The chemical shift extrapolated to infinitely dilute TPARF in benzene was 346.8 ppm, compared to 346.1 ppm obtained at our highest solution NMR concentration of 7 mM. In the presence of DBAP, the chemical shift extrapolated to infinite dilution was 349.7 ppm, indistinguishable from the 349.8 ppm chemical shift at our highest solution NMR concentration. That DBAP blocks the associations between flavins indicates that these associations employ the same functionalities as those engaged by DBAP, consistent with coplanar flavins H-bonding via O2, N3H, and O4 (modeled in Supporting Information Figure 7S). This also agrees with Moonen's report that TARF in chloroform forms H-bonding interactions at high concentration that are prevented by methylation at N3.[64] Therein, TARF was found to dimerize via the O2−N3H−O4 edge, and this produced a slight upfield shift in the chemical shift of N5,[64] as we report here. Thus, we conclude that in concentrated solution our TPARF exists substantially as dimers formed via interactions involving O2, N3H, and O4.

To assess the size of the effect on the CSPVs, we turned to DFT because SSNMR is not sufficiently sensitive to permit accurate CSPV determinations on diluted TPARF samples. We generated the four most plausible H-bonding flavin dimers and subjected them to geometry optimization. Three achieved low-energy minima. The dimers' energies indicated that one dimer would predominate in a Boltzmann-weighted population but that two others would nonetheless contribute 3% or more of the population (Supporting Information, Table 4S). Supporting Information Table 4S shows the chemical shifts and energy calculated for each dimer. The energies were used to calculate the fraction of the population expected to occur in each configuration at −60 °C, and these populations were used to calculate a Boltzmann-weighted population average set of CSPVs and $\delta_{iso}$.

The calculated Boltzmann-weighted average isotropic chemical shift of the LF dimer differed from that of monomeric LF by having a 0.6 ppm lower $\delta_{iso}$. This agrees within error with the experimental finding of a 0.7 ppm lower $\delta_{iso}$ in concentrated solution, supporting the validity of the calculations and indicating that our Boltzmann-weighted population of dimers is a satisfactory model for the state of TPARF in our high-concentration solutions. Therefore, we used the Boltzmann-weighted average flavin dimer chemical shifts as our reference values for TPARF alone in benzene (Table 1 and Table 4S, Supporting Information).

The above calculations indicate that LF dimerization produces a change of −1 ppm for $\delta_{11}$ and changes of −1 and 0 ppm for $\delta_{22}$ and $\delta_{33}$, respectively (Supporting Information, Table 4S). These corrections are small relative to our experimental errors and

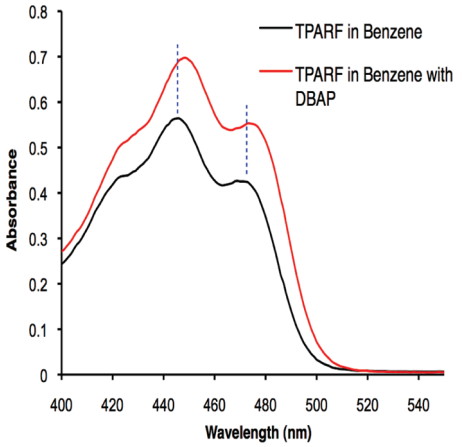


**Figure 1.** Optical spectrum of TPARF in benzene and effects of complexation with DBAP.

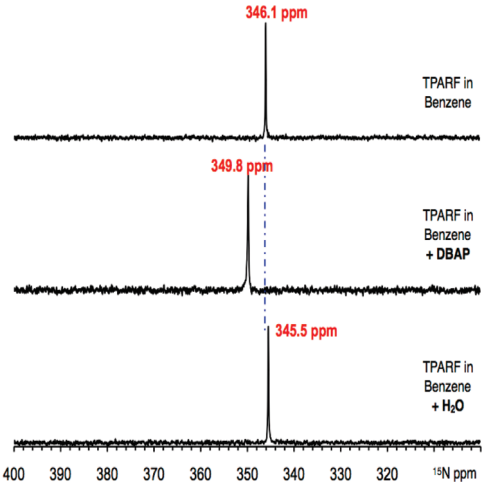


**Figure 2.** Solution NMR spectra of $^{15}$N-N5−TPARF in benzene, alone, or with added saturating DBAP or water (5 stoichiometric equivalents).

therefore have relatively minor significance to the quantitative conclusions we may draw. However the above studies affect our interpretation of the results that follow, as they suggest that the experimental CSPV changes we document below should be interpreted as the results of dissociation of flavin dimers in addition to the formation of new H-bonds with the added H-bonding partner(s). We note that the subtlety of the optical and NMR signatures of TPARF self-association indicates that this has relatively minor effects on flavin electronic structure, so the majority of the effects observed can still be interpreted as substantially consequences of the new interactions with the added H-bonding partner.

**3.2. Effects of Temperature and Freezing.** Another requirement for SSNMR is that solutions be frozen. This introduces both the effects of the state change from liquid to solid and the lower temperature. The effects are not negligible. The $\delta_{iso}$ of TPARF in benzene at −60 °C was 342.0 ± 0.4 ppm, whereas $\delta_{iso}$ measured in solution at room temperature was 346.1 ppm.[66] To evaluate the effect of temperature alone, we compared the $\delta_{iso}$ and CSPV of TPARF powder at room temperature and −60 °C. At room temperature, $\delta_{iso}$ was found to be 342.1 ± 0.2 ppm, whereas the same sample at −60 °C displayed a $\delta_{iso}$ of 342.8 ppm. TPARF in benzene at −60 °C also had a similar $\delta_{iso}$ of 342.0 ± 0.4 ppm. Thus, the solid nature of our SSNMR samples appears responsible for the large difference between the $\delta_{iso}$ obtained in solution and those obtained by SSNMR. We were not able to find conditions for forming glasses, even using mixtures of benzene with toluene, so our TPARF likely finds itself in microscopic domains of various high concentrations, upon freezing. Indeed the $\delta_{iso}$ and CSPVs for TPARF frozen to −60 °C in benzene were not significantly different from those of powdered TPARF at −60 °C (Figure 3 and Supporting Information, Table 5S). However, since the H-bonding partners DBAP and water should be concentrated likewise, the ability of DBAP or water to compete with flavin dimerization should be retained, and the data that follow support this.

**3.3. Observation of TPARF's Complex with DBAP.** TPARF in benzene had a maximum absorbance at 445 nm. Addition of DBAP to TPARF in benzene resulted in a 20% increase in the extinction coefficient of the flavin in concert with a red shift of the main absorption band from 445 to 447 nm, in agreement with published work[46] (Figure 1). This and the previous study of the electrochemical potentials of TPARF alone and in complexes show that this model system behaves similarly to the traditional TARF model system.[44]

In solution NMR spectra, the $\delta_{iso}$ of TPARF's N5 increased by 3.7 ppm upon H-bonding with DBAP (Figure 2). This is a significant change but small compared to the changes observed by SSNMR.

For TPARF in benzene, $^{15}$N one-dimensional cross-polarized magic angle spinning SSNMR spectra (CP-MAS spectra) showed that the signal spans 716 ppm with a $\delta_{iso}$ of 342.0 ppm (Table 1 and Figure 3). The three CSPVs are 676 ± 3, 390 ± 2, and −40 ± 6 ppm based on determination of the CSPVs at three different MAS speeds as well as replicate determinations on replicate samples.

To study the complex with DBAP, we added saturating DBAP[67] to TPARF in benzene and froze the sample to achieve the solid state. Upon complexation with DBAP, TPARF's N5 $\delta_{iso}$ increased 6.7 ± 0.9 ppm (Table 1). Of the three CSPVs, $\delta_{11}$ was the most responsive to the H-bonding, with a change of 10 ± 5 ppm (Tables 1 and 2). $\delta_{11}$'s strong deshielding and responsiveness to noncovalent interactions are expected based on prior experiments and calculations on simpler systems.[29,43] However, our experimental results extend these findings to the more complex and biologically important flavin system. Furthermore, previous studies addressed direct interactions with the observed atom, whereas DBAP does not form a H-bond with N5 and must exert its effect via perturbation of molecular orbitals.[68] Nonetheless, the changes in $\delta_{iso}$ and $\delta_{11}$ are readily detected even at 40 MHz (for $^{15}$N) and are significant compared with experimental error. Thus, we anticipate that it should be possible to detect the effects on N5 of H-bonding between proteins and flavins.

**3.4. Observation of TPARF's H-bonding with Water.** There has not been a synthetic binding partner designed to H-bond to N5, in part because H-bond donation to N5 is less common in proteins. However, the flavin N5 can form H-bonds with $H_2O$ molecules. In solution NMR spectra, the presence of 5 equivalents of $H_2O$ produced a $\delta_{iso}$ of 342.5 ± 0.3 ppm (Figure 2), barely changed from TPARF in benzene alone at 342.0 ± 0.3 ppm. This contrasts with a 10 ppm difference reported between the N5 $\delta_{iso}$ of FMN in $H_2O$ and the N5 of TARF in $CHCl_3$.[64] However, in that case the bulk dielectrics of the two media were very different (78 vs 5), whereas in our case the bulk dielectric is not expected

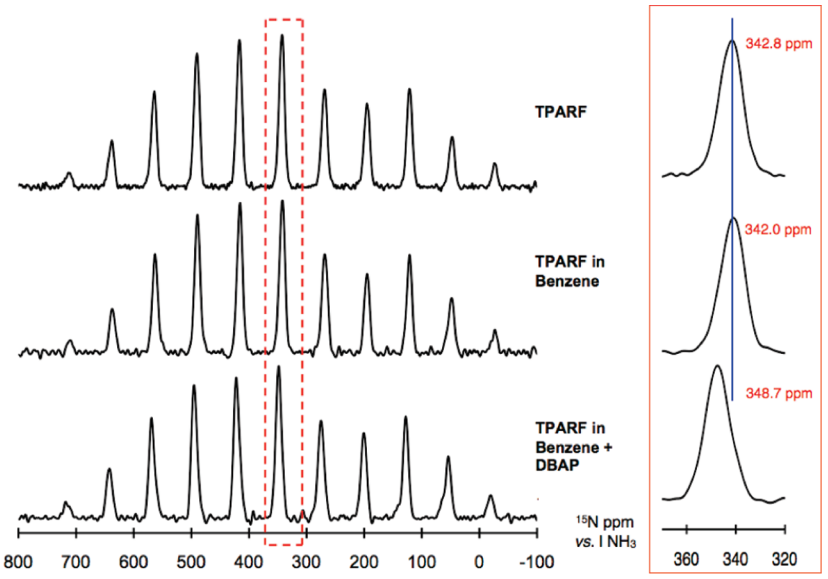


**Figure 3.** Comparison of the $^{15}$N CP-MAS spectra of dry [$^{15}$N-N5] TPARF, [$^{15}$N-N5] TPARF in benzene, and [$^{15}$N-N5] TPARF in benzene saturated with DBAP, all at a MAS speed of 3000 Hz. (Central peaks in the red box are enlarged for comparison of the $\delta_{iso}$s.)

**Table 2. Effects of H-Bonding Partners on Experimental $^{15}$N CSPVs of N5 of TPARF and Analogous Calculated CSPVs of LF[a]**

| change | | $\delta_{11}$ (ppm) | $\delta_{22}$ (ppm) | $\delta_{33}$ (ppm) | $\delta_{iso}$ (ppm) |
|---|---|---|---|---|---|
| effect of DBAP | exptl | 10 ± 5 | 5 ± 5 | 4 ± 7 | 6.7 ± 0.9 |
| | calcd | 12 | 3 | 0 | 4.7 |
| effect of $H_2O$ | exptl | −6 ± 4 | 1 ± 4 | 6 ± 7 | 0.5 ± 0.5 |
| | calcd | −5 | 1 | 0 | −1 |

[a] Geometry optimization and GIAO chemical shift calculations employed B3PW91 with the 6-311++G(2d,2p) basis set. Experimental values are accompanied by standard deviations propagated from those in Table 1. For comparison, replicate determinations of the CSPVs of TPARF alone on separate occasions and different samples produced CSPVs that differed from one another by 2, 3, and 3 ppm for $\delta_{11}$, $\delta_{22}$, and $\delta_{33}$, respectively, and $\delta_{iso}$ values that differed by 0.6 ppm

to change greatly upon addition of 1.6 $\mu$L of $H_2O$ to 80 $\mu$L of benzene. Nevertheless, the CSPVs measured by SSNMR revealed that the added $H_2O$ perturbs the flavin electronic structure, as $\delta_{11}$ changed by −6 ± 4 ppm. (Note the changes in intensity distribution among spinning side bands in Supporting Information Figure 10S.) The SSNMR spectra of this sample were experimentally indistinguishable from those obtained upon addition of 15 stoichiometric equivalents of water, indicating that $H_2O$ in excess of 5 equiv produces negligible additional effects (Supporting Information Figure 10S). Thus, although chemical shift changes are insignificant by solution NMR, SSNMR detects a significant effect on $\delta_{11}$. Moreover, $H_2O$'s effect on the SSNMR signal is qualitatively distinct from the effect of H-bonding with DBAP, with $\delta_{11}$ decreasing instead of increasing and $\delta_{iso}$ barely changing instead of increasing (Table 2). These contrasting responses demonstrate that SSNMR can distinguish among different types or arrangements of H-bonds.

**3.5. Computations of the TPARF Complex with DBAP.** The experimental changes could be replicated computationally. The geometries of oxidized lumiflavin (LF), LF dimers ($LF_2$), and the complex of LF and DBAP were optimized using density functional theory (DFT) and the B3PW91 functional[69] with the 6-311++G(2d,2p) basis set and SCRF. While a different functional and smaller basis sets have been used for similar efforts, we found that higher levels of theory were needed to achieve energy convergence and optimal agreement with experimental results, as shown in the Supporting Information (Figures 1S and 2S).[70] The calculated $\delta_{iso}$ for N5 of $LF_2$ is 362 ppm, 20 ppm larger than the experimental value at −60 °C. The CSPVs are 722, 398, and −33 ppm, respectively. These differ from the experimental values by 46, 8, and 7 ppm, respectively. For comparison, deviations between calculated and observed CSPVs of 40, 1, and 13 ppm were obtained for pyridine, in the rigorous study of Solum et al.[29] Wei et al. report differences of 35, 56, and −3 for the principal values of the protonated N of imidazole.[38] Thus, our calculations achieve a level of agreement with experiment that is comparable to that achieved in other published works. Moreover, very similar differences between calculation and experiment were observed for the complex of TPARF with DBAP (47, 6, and 3 ppm, respectively, Table 1). Therefore, these differences are likely due substantially to complications inherent to calculations on molecules as large and highly correlated as ours and imperfect accounting for solvent effects and/or temperature effects. Moreover our calculated chemical shift for $NH_3$ is only 3 ppm from that of gaseous $NH_3$, implicating the complicated natures of our samples rather than the computations per se.[59] However, such issues should not affect *changes* in chemical shifts. Indeed, it is very common for authors to report differences between pairs of chemical shift principal values rather than individual values.

The *changes* in chemical shifts calculated upon H-bond formation agreed very well with *changes* in experimental values (Table 2). Thus, our calculated change in $\delta_{iso}$ due to H-bonding with DBAP deviates from the experimental value by 2 ppm, which at an NMR frequency of 40 MHz corresponds to an energy of 80 Hz. In comparison, the disparity between observed and calculated changes in vibrational frequencies upon ionization of lumazine was on the order of 3 $cm^{-1}$ = 9 × $10^{10}$ Hz.[71] Thus, our calculations do very well in reproducing experimental *changes*. Moreover since our purpose is to understand *changes* in flavin

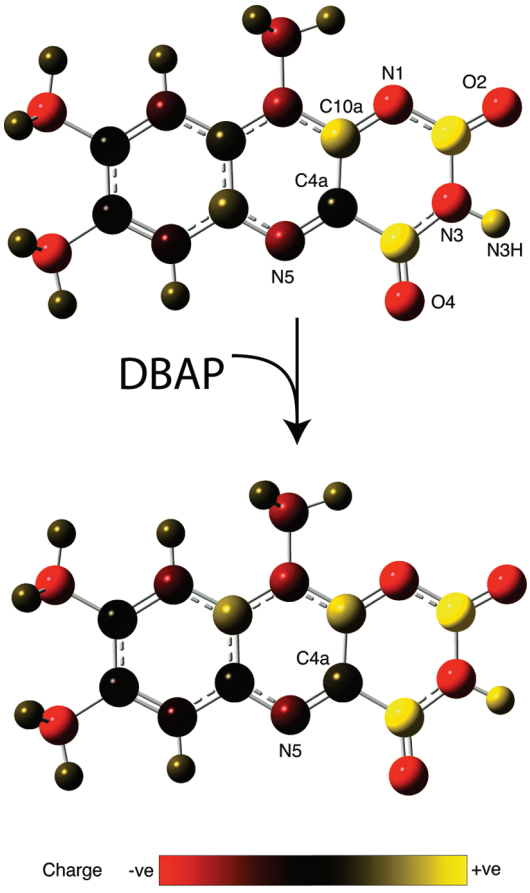


**Figure 4.** Distribution of NPA electron density in LF (top) and LF complexed with DBAP (bottom). The total charge of LF changed from 0.01 to 0.04 upon complexation with DBAP. Structures are oriented as in Scheme 1: red indicates excess electron density, and yellow indicates electron deficiency.

reactivity brought about by interactions with proteins, it is the *changes* in CSPVs produced by H-bonding that are most important.

Upon H-bonding with DBAP, the calculated CSPVs changed by 12, 3, and 0 ppm, respectively. Besides agreeing within error with our experimental changes, these calculations confirm that $\delta_{11}$ is considerably more responsive to H-bonding with DBAP than the other CSPVs or $\delta_{iso}$.

**3.6. Implications for Electronic Structure.** The qualitative as well as quantitative agreement between our calculations and experiments indicates that the calculations are able to capture changes in flavin electronic structure produced by complexation with DBAP (upon displacement of a partner LF). Therefore, we can use the calculated electronic structures to understand the effect of DBAP binding on reactivity. The natural population analysis (NPA) distributions of electron density in LF and LF·DBAP indicate that the most positive atom is C2, consistent with its double bond to O and two bonds to N, and the most negative atoms are N3, N1, and O2 consistent with their electronegative natures (Figure 4). Complexation with DBAP did not significantly change this very strong polarization of bonds within the uracyl ring. However, the flavin ring propagates the effects of H-bonding to more distant sites. Comparing the effects of complexation on the redox-active (N5, C4a, C10a, N1) diazabutadiene system with the effects on sites directly involved in H-bonding (C2, N3H, C4) and sites at the far end of the flavin (C7, C7a, C8, C8a), we find changes in excess charge of 0.10 ± 0.04 in the diazabutadiene system, whereas the changes at sites directly involved in H-bonding and at the far end of the flavin are both comparable to the uncertainty. For N5 plus C4a, the two sites associated with most flavin reactivity, binding to DBAP produces a 0.12 ± 0.04 increase in net charge equivalent to depletion of 12% of an electron equivalent. These results are consistent with the measured 100 mV increase in TPARF's reduction midpoint potential upon complexation with DBAP.[46]

The counterpoise-corrected energy of LF·DBAP complex formation was −27 kJ/mol.[62] Considering that it does not take into account entropic contributions or solvation effects, this value is consistent with the standard-state Gibbs free energy of −19.2 kJ/mol calculated from the 420 $\mu$M dissociation constant of TPARF and DBAP in benzene.[46] These values imply H-bond energies on the order of 10 kJ/mol each, consistent with the good computed bond geometries and distances of 2.9−3.0 Å between participating N or O atoms (Supporting Information Figure 8S). Thus, calculated properties of the complex are mutually consistent and consistent with observed reactivity and interactions. Nonetheless, the natures of the flavin-based HOMO and LUMO do not change substantially upon complexation of DBAP (Supporting Information Figure 9S). Indeed, the four HOMOs and the four LUMOs are qualitatively the same for LF·DBAP as for LF, although HOMO-2 and HOMO-3 exchange positions in the energy order upon complexation with either DBAP or water. Thus, we do not expect a large change in the nature of the reactivity of the oxidized state, consistent with experiment.

**3.7. Computation of the TPARF Complex with Water.** DBAP forms a chelate-like interaction with TPARF that favors formation of a unique complex. In contrast, H-bonds with $H_2O$ are much less site-specific. We performed calculations starting with a single water at numerous positions around the flavin ring, as well as analogous calculations with two waters, three, four, and up to eight water molecules in addition to LF. Our calculations found that LF can bind $H_2O$ molecules at a variety of different positions, which moreover depend on the locations of other $H_2O$ molecules, as anticipated (Supporting Information Figures 10S and 11S). Thus, we can expect that individual $H_2O$ molecules may fluctuate between binding in different locations and being detached from the flavin, so that an ensemble of flavin molecules with a few $H_2O$ each will include a statistical collection of all the different possible H-bonding options for each $H_2O$ molecule.

CSPVs and energies were calculated for all the distinct minimized one-water configurations (four) and all the distinct two-water configurations (six). The general lack of agreement between experiment and individual calculations, wherein calculated $\delta_{11}$ values were scattered widely above and below the experimental value, indicates that the sample of TPARF and $H_2O$ is not well described by any one configuration of H-bonded $H_2O$ (Figure 5). The lack of improvement as the number of water molecules in the calculation was increased (Supporting Information Figure 13S) could be explained by the fact that when more waters were present they tended to interact among themselves rather than interact with all the functionalities of the flavin. Thus, we observed a tendency to partition, rather than solvate, the LF (Supporting Information Figure 12S). The calculations of individual one-water (and two-water) configurations demonstrated that when $H_2O$ H-bonded directly with N5 both $\delta_{11}$ and $\delta_{iso}$ decreased a lot (−50 and −17 ppm, respectively, Figure 5 and Supporting Information Figure 13S), whereas when

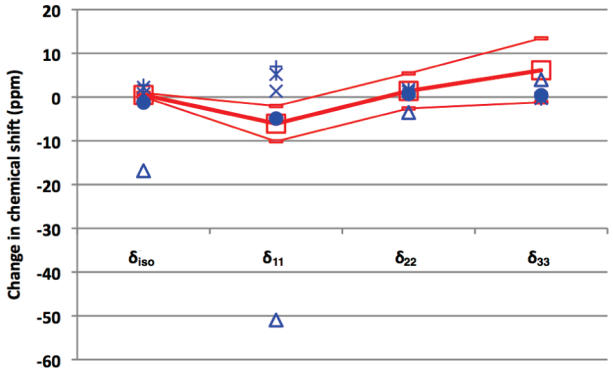


**Figure 5.** Changes in GIAO NMR CSPVs and $\delta_{iso}$ calculated from optimized LF·$H_2O$ complexes. The configuration with a water H-bonding to N5 (Δ) yielded a large decrease in $\delta_{11}$, whereas the configurations with water H-bonding to different positions (×, ∗, +) yielded increases in $\delta_{11}$. Boltzmann-weighted averages of the shifts of single-water configurations are in filled circles, ●. The red □s denote the experimental changes in chemical shift upon addition of water, and the associated experimental errors are used to generate error margins shown as dashes connected by lines. Calculated results that fall between these errors can be considered to be in agreement with experiment.

$H_2O$ formed H-bonds with atoms other than N5, $\delta_{11}$ and $\delta_{iso}$ increased (by average increases of 5 and 2 ppm, respectively). The same trends were observed with larger numbers of waters too. The fact that the experimental changes of −6 and 0.5 ppm were intermediate between these two categories supports an approach that combines the effects of multiple different H-bonding configurations, at once.

Boltzmann-weighted averages of CSPVs produced by the four single-water configurations agreed with experiment within error (Figure 5), although the Boltzmann average $\delta_{iso}$ was 1.7 ppm from the experimental value (0.5 ± 0.5). The two-water Boltzmann average $\delta_{iso}$ was somewhat closer to the experimental value but still outside error. Given our errors and the relative naivety of the models, it is not meaningful to distinguish between these models; however, it is clear that both are substantial improvements over individual configurations (Figure 5 and Supporting Information, Figure 13S). The Boltzmann-weighted averages reproduced the observations that $\delta_{11}$ decreased upon addition of water, while the change in $\delta_{iso}$ was very slight. This contrasts with the significant increase in $\delta_{11}$ and $\delta_{iso}$ produced by binding to DBAP. Thus, our calculations reproduce the qualitative differences between the effects of H-bonding with DBAP vs water, and models of greater complexity are not justified.

Counterpoise-corrected energies of binding between LF and one water ranged from −25 to −30 kJ/mol. These energies reflect the formation of two H-bonds per water molecule in most cases, water's characteristically strong H-bonds, and its greater freedom than DBAP to adopt the position that optimizes individual H-bonds. However, the values we obtain are in reasonable agreement with the literature (up to 20 kJ/mol for the Gibbs free energy).[72] Thus, our NMR-validated calculations again yield properties that agree with observed chemical behavior.

In summary, the competition between various sites on LF that have comparable affinities for water conspires with cancellation of contributions from the different CSPVs to produce a very small net effect on the $\delta_{iso}$. However, the individual CSPVs are more responsive to water, and the effect on $\delta_{11}$ is both experimentally significant and consistent with a contribution from water H-bonded to N5.[29,30] Even for this more complicated case, our experiments demonstrate that SSNMR provides added sensitivity to noncovalent interactions that will greatly advance our ability to detect and distinguish interactions in proteins that tune flavin reactivity.

## 4. DISCUSSION

Many cofactors are activated for a particular reaction when bound in an enzyme active site, and some even require that substrates be bound as well.[73−75] The sensitivity of CSPVs, especially those of the pyridine-type of N atoms within the oxidized flavin's conjugated ring system, makes them ideal probes of perturbations of the cofactor's electronic structure that may be produced by interactions with the protein.[76] Many organic cofactors include conjugated heterocycles, for example, pterins, nicotinamide adenine dinucleotide, thiamine, pyridoxal/amine phosphate, and biotin, in addition to flavins. We speculate that the smaller energy spacing between the HOMOs and the LUMOs that results from incorporation of heteroatoms in the $\pi$ system may form a basis for evolution's selection of heterocyclic cofactors, in addition to their ready production from the simple precursors early life would have had access to.[77,78] Indeed, it is likely that the cofactors we have today are a few of many molecules that once acted alone, without enveloping proteins, to catalyze early biological reactions. They may thus constitute a window on our deep evolutionary biochemical past. The approach we demonstrate here should be applicable and fruitful for many of them.[41,42]

We have shown that the $^{15}N$ CSPVs not only respond to H-bonding but also display qualitatively different responses to different sorts of H-bonding. These findings imply that different protein active sites may produce different changes in the CSPVs of a bound flavin. Because our calculations reproduce these differences, they suggest that given an active site one could perform DFT calculations on the bound flavin and protein environment and use SSNMR as a critical test of the validity of the calculation. This would be a convincing test based on our demonstration that the three CSPVs of SSNMR afford diverse responses that can distinguish between different modes of H-bonding and thus different models of a binding site. Given the success of our current calculations, we have begun computing effects on CSPVs expected from different interactions observed in protein active sites, to learn whether they may be associated with sufficiently distinct NMR signatures and to determine which flavin ring atoms will be the best positions to observe. Positionally specific isotopic labeling can be achieved via synthetic[47] or biosynthetic means.[79] A carefully chosen set of positions may be able to provide insight into the environment of the flavin even in the absence of a crystal structure.

Spectroscopically validated calculations would also greatly increase the value of the NMR results. For the current case of N5, a large decrease in $\delta_{11}$ in conjunction with a small increase in $\delta_{33}$ can now be taken as evidence for acceptance of an H-bond by N5 (although other interactions may also be found to produce similar effects).

H-bonds donated to N1, O2, and O4 have been reported to draw electron density out of the flavin and make it a better oxidant.[80] Indeed, our spectroscopically validated calculations find that the redox-active diazabutadiene system becomes less net-negative, consistent with the observed increase in reduction

midpoint potential, even though electron density is little changed at the actual sites of H-bonding. Thus, our calculations are consistent with experimental findings that complexation with DBAP increases the midpoint potential observed for one-electron reduction of TPARF in benzene by 100 mV,[46] similar to the 150 mV increase observed for analogous model systems[44] and the 170 mV increase in the one-electron reduction potential of FMN upon binding to flavodoxin.[81,82] This suggests that NMR-validated calculations may prove useful for understanding reactivity and possibly even predicting it.

In the current two cases, electronic effects were subtle, possibly because we were replacing one H-bonding interaction with another one, rather than generating H-bonds in a system that had none beforehand.[83] In addition, the N5 atom we observed is several bonds away from the closest point of contact with the H-bonding partner DBAP, so the changes in CSPV we detected are indirect, propagated by the flavin molecular orbitals over several bonds. This can explain the apparent contrast between the 10 ppm changes to $\delta_{11}$ observed here and the 40 ppm calculated effect on $\delta_{11}$ of H-bonding to the N of benzamide reported by Facelli,[84] or the 50 ppm decrease we calculate when a $H_2O$ H-bonds directly to N5. Thus, an interaction that targetted N5 would be expected to produce a larger effect. Although H-bonding with water appears to include H-bonding to N5, our calculations and experiments indicate that this represents only a relatively small fraction of the ensemble of configurations present, explaining why this effect too is relatively modest in our experimental model.

In addition, the complexes with DBAP and water were both favorable and relatively weak. A favorable interaction would most simply stabilize the existing state rather than change it. Nevertheless, significant changes in CSPVs indicate that there were repercussions for the flavin electronic structure, as we could detect the effects of H-bonds formed at remote positions. For FMN and FAD bound in proteins, where binding can be very tight and exploit interactions with the ribose (adenine) and phosphate moieties as bases for affinity, the flavin-binding site can divert some binding energy to distortion of the flavin and its electronic structure. Indeed, larger solution NMR changes are observed upon flavin binding to proteins[24] than upon binding to DBAP. Thus, larger effects are expected in SSNMR as well, and those we document here on models underestimate what is possible in proteins and thereby provide a stringent proof of principle that SSNMR should be able to perceive perturbations applied by proteins.

## 5. CONCLUSIONS

The foregoing demonstrates that $^{15}N$ SSNMR CSPVs can sense even remote and statistical perturbations of flavins upon formation of H-bonds, even when the effects are barely discernible via solution NMR. SSNMR CSPVs can be used to validate DFT calculations that in turn permit interpretation of the CSPVs in terms of the nature of the electronic changes that result from different H-bonding interactions. Due to the high responsiveness of NMR and the existence of numerous potential probe sites in the flavin ring system, this approach provides a uniquely perceptive and appropriate means of studying modulations of flavin electronic structure that may underlie different reactivities observed in different enzymes. The same principles apply to several other widespread organic cofactors. Thus, we anticipate that SSNMR-validated DFT computation can provide a general approach to understanding how proteins tune the reactivity of organic cofactors at a fundamental and unifying level. Such an understanding would open up immense possibilities for modifying the reactivity of enzymes by modifying their interfaces with their cofactors. Thus the approach we describe here advances efforts to understand the biochemical economy of enzymes and to manipulate the versatile cofactors upon which it rests.

## ■ ASSOCIATED CONTENT

**Supporting Information.** Thirteen figures and five tables in total: A table of individual results: CSPV values obtained at different MAS speeds; two tables of Cartesian coordinates, for geometry-optimized LF and the LF·DBAP complex; details regarding NMR data acquisition; details of choices of level of computational theory including demonstration of basis set saturation for both geometry optimization and chemical shift tensor calculation as well as comparison of the performance of two different density functionals (2 figures); explanation of approaches used to estimate the uncertainty associated with computational results (2 figures); data on concentration dependence of TPARF's optical signal and N5 isotropic chemical shift (2 figures); figure and tables providing computational evidence pertinent to possible flavin dimerization (1 figure and 2 tables); table showing the temperature dependence of CSPVs (1 table); figure with H-bonding distances obtained for the LF·DBAP complex and for a complex between LF and five waters (the one in which water displayed an H-bond with N5); four highest-energy occupied MOs and four lowest-energy unoccupied LF MOs for each of LF and LF in complex with DBAP (one figure); SSNMR spectra of TPARF in dry benzene before and after addition of water (one figure); details of considerations and methods used to explore and treat the interactions between water and LF computationally (3 figures). This material is available free of charge via the Internet at http://pubs.acs.org.

## ■ AUTHOR INFORMATION

### Corresponding Author

*Tel.: (859) 257-9349. Fax: (859) 323-1069. E-mail: afm@uky.edu.

### Present Addresses

[#]Department of Physics, The City College of New York, New York, NY 10031, USA.

[¶]Department of Chemistry and Biochemistry, 9500 Gilman Drive, University of California, San Diego, La Jolla, CA 92093-0332.

## ■ ACKNOWLEDGMENT

We thank Mssrs. A. Sebesta and W. J. Layton for assistance with NMR spectrometer upkeep, Mssrs J. Morris, C. Tipson and H. Meekins for custom machining, Dr. R. M. Sheetz for help with supercomputer access, Dr. C. Moser for help with figures, and Dr. Ilya Kuprov (Durham University) for advice regarding calculations. We gratefully acknowledge the Research Challenge Trust Fund of Kentucky for support to D. Cui and A.-F. Miller, the Petroleum Research Fund for support to A.-F. Miller under 44321-AC4, and the National Institutes of Health for support to P. L. Dutton via GM 41048. The 400 MHz NMR spectrometer used for SSNMR experiments was purchased with funding from the National Science Foundation obtained under the MRI

program Grant # DMR-9977388. Supercomputer access was obtained via allocation CHE020054 from the N.CSA and courtesy of the CCS of the University of Kentucky. We also thank an anonymous reviewer for detailed comments.

## REFERENCES

(1) Abbreviations: BSSE, basis set superposition error; calcd, calculated; CP, cross polarization; CSPVs, chemical shift tensor principle values; DBAP, dibenzylamidopyridine; DFT, density functional theory; exptl, experimental; FAD, flavin adenine dinucleotide; FMN, flavin mononucleotide; GIAO, gauge including atomic orbitals; H-bond, hydrogen bond; LF, lumiflavin; MAS, magic angle spinning; MD, molecular dynamics; NBO, natural bond order; NPA, natural population analysis; SSNMR, solid state NMR; TARF, tetraacetylriboflavin; TPARF, tetraphenylacetylriboflavin.

(2) Massey, V. *Biochem. Soc. Trans.* **2000**, *28*, 283–296.

(3) Fraaije, M. W.; Mattevi, A. *TIBS* **2000**, *25*, 126–132.

(4) Massey, V.; Hemmerich, P. *Biochem. Soc. Trans.* **1980**, *8*, 246–257.

(5) Walsh, J. D.; Miller, A.-F. *J. Mol. Struct. (Theochem)* **2003**, *623*, 185–195.

(6) Lennon, B. W.; Williams, C. H., Jr.; Ludwig, M. L. *Protein Sci.* **1999**, *8*, 2366–2379.

(7) Koder, R. L.; Haynes, C. A.; Rodgers, M. E.; Rodgers, D. W.; Miller, A.-F. *Biochemistry* **2002**, *41*, 14197–14205.

(8) Talfournier, F.; Munro, A. W.; Basran, J.; Sutcliffe, M. J.; Daff, S.; Chapman, S. K.; Scrutton, N. S. *J. Biol. Chem.* **2001**, *276*, 20190–20196.

(9) Zhou, Z.; Swenson, R. P. *Biochemistry* **1996**, *35*, 15980–15988.

(10) Breinlinger, E. C.; Rotello, V. M. *J. Am. Chem. Soc.* **1997**, *119*, 1165–1166.

(11) Lostao, A.; Gomez-Moreno, C.; Mayhew, S. G.; Sancho, J. *Biochemistry* **1997**, *36*, 14334–14344.

(12) Schopfer, L. M.; Ludwig, M. L.; Massey, V. In *Flavins and Flavoproteins 1990*; Curti, B., Ronchi, S., Zanetti, G., Eds.; Walter de Güyter: Berlin, 1991; pp 399−404.

(13) Krishnan, N.; Becker, D. F. *Biochemistry* **2005**, *44*, 9130–9139.

(14) Chang, F. C.; Bradley, L. H.; Swenson, R. P. *Biochim. Biophys. Acta, Bioenerg.* **2001**, *1504*, 319–328.

(15) Cuello, A. O.; McIntosh, C. M.; Rotello, V. M. *J. Am. Chem. Soc.* **2000**, *122*, 3517–3521.

(16) Bradley, L. H.; Swenson, R. P. *Biochemistry* **2001**, *40*, 8686–8695.

(17) Kraft, B. J.; Masuda, S.; Kikuchi, J.; Dragnea, V.; Tollin, G.; Zaleski, J. M.; Bauer, C. E. *Biochemistry* **2003**, *42*, 6726–6734.

(18) Lin, L. Y.-C.; Szittner, R.; Friedman, R.; Meighen, E. A. *Biochemistry* **2004**, *43*, 3183–3194.

(19) Miller, A.-F.; Koder, R. L., Jr.; Walsh, J. D.; Haynes, C. A.; Rodgers, M.; Erdmann, H.; Hecht, H.-J.; Rodgers, D. W. In *Flavins and flavoproteins 2002*; Scrutton, N. S., Chapman, S. K., Eds.; Rudolf Weber: Berlin, 2002; pp 293−298.

(20) Kodali, G.; Siddiqui, S. U.; Stanley, R. J. *J. Am. Chem. Soc.* **2009**, *131*, 4795–4807.

(21) Hopkins, N.; Stanley, R. J. *Biochemistry* **2003**, *42*, 991–999.

(22) Yang, K. Y.; Swenson, R. P. *Biochemistry* **2007**, *46*, 2289–2297.

(23) Nishina, Y.; Sato, K.; Setoyama, C.; Tamaoki, H.; Miura, R.; Shiga, K. *J. Biochem.* **2007**, *142*, 265–272.

(24) Müller, F. In *Chemistry and biochemistry of flavoenzymes*; Müller, F., Ed.; C.R.C.: Boca Raton Fl., 1992; Vol. III, pp 558−595.

(25) Eisenreich, W.; Kemter, K.; Bacher, A.; Mulrooney, S. B.; Williams, C. h.; Müller, F. *Eur. J. Biochem.* **2004**, *271*, 1437–1452.

(26) Rüterjans, H.; Fleischmann, G.; Löhr, M.; Knauf, F.; Blümel, M.; Lederer, F.; Mayhew, S. G.; Müller, F. *Biochem. Soc. Trans.* **1996**, *24*, 116–121.

(27) The term "chemical shift anisotropy" or CSA has been used in a general way to describe the components of chemical shift that augment the isotropic value when the object of NMR study is not free to reorient, or specifically $\delta_{11} - (\delta_{33}+\delta_{22})/2$, where the $\delta$ values are the principal values of either the chemical shift anisotropy tensor or the chemical shift tensor. Because the current work discusses the values of individual chemical shift tensor principal values, we employ the term "chemical shift (tensor) principal value" or CSPV, instead.

(28) We follow the convention that the least shielded principal value is named $\delta_{11}$ and the most shielded one is named $\delta_{33}$.

(29) Solum, M. S.; Altmann, K. L.; Strohmeier, M.; Berges, D. A.; Zhang, Y.; Facelli, J. C.; Pugmire, R. J.; Grant, D. M. *J. Am. Chem. Soc.* **1997**, *119*, 9804–9809.

(30) Koder, R. L., Jr.; Walsh, J. D.; Pometun, M. S.; Dutton, P. L.; Wittebort, R. J.; Miller, A.-F. *J. Am. Chem. Soc.* **2006**, *128*, 15200–15208.

(31) Ramsey, N. F. *Phys. Rev.* **1950**, *78*, 699–703.

(32) Lumsden, M. D.; Wu, G.; Wasylishen, R. E.; Curtis, R. D. *J. Am. Chem. Soc.* **1993**, *115*, 2825–2832.

(33) Salzmann, R.; Wojdelski, M.; McMahon, M.; Havlin, R. H.; Oldfield, E. *J. Am. Chem. Soc.* **1998**, *120*, 1349–1356.

(34) For the purposes of this paper, HOMO denotes several highest-lying occupied molecular orbitals, not just the one that lies highest of all, as symmetry and localization differences can be as important as the energy in determining which HOMO is reactive. Similarly, LUMO denotes several lowest-lying unoccupied molecular orbitals.

(35) Waddell, K. W.; Chekmenev, E.; Wittebort, R. J. *J. Am. Chem. Soc.* **2005**, *127*, 9030–9035.

(36) Yao, L.; Grishaev, A.; Cornilescu, G.; Bax, A. *J. Am. Chem. Soc.* **2010**, *132*, 4295–4309.

(37) Marassi, F. M.; Opella, S. J. *J. Magn. Reson.* **2000**, *144*, 150.

(38) Wei, Y.; de Dios, A. C.; McDermott, A. E. *J. Am. Chem. Soc.* **1999**, *121*, 10389–10394.

(39) Hu, F.; Luo, W.; Hong, M. *Science* **2010**, *330*, 505–508.

(40) Sauve, A. A.; M., C. S.; Zech, S. G.; Basso, L. A.; Lewandowicz, A.; Santos, D. S.; Grubmeyer, C.; Evans, G. B.; Furneaux, R. H.; Tyler, P. C.; McDermott, A.; Girvin, M. E.; Schramm, V. L. *Biochemistry* **2003**, *42*, 5694–5605.

(41) Lai, J.; Niks, D.; Wang, Y.; Domratcheva, T.; Barends, T. R. M.; Schwarz, F.; Olsen, R. A.; Elliott, D. W.; Fatmi, M. Q.; Chang, C. A.; Schlichting, I.; Dunn, M. F.; Mueller, L. J. *J. Am. Chem. Soc.* **2011**, *133*, 4–7.

(42) Paramasivam, S.; Balakrishnan, A.; Dmitrenko, O.; Godert, A.; Begley, T. P.; Jordan, F.; Polenova, T. *J. Phys. Chem. B* **2011**, *115*, 730–736.

(43) Walsh, J. D.; Miller, A.-F. *J. Phys. Chem. B* **2003**, *107*, 854–863.

(44) Breinlinger, E.; Niemz, A.; Rotello, V. M. *J. Am. Chem. Soc.* **1995**, *117*, 5379–5380.

(45) Walsh, J. D. Doctoral, The Johns Hopkins Universisty, 2003.

(46) Cerda, J. F.; Koder, R. L., Jr.; Lichtenstein, B. R.; Moser, C. M.; Miller, A.-F.; Dutton, P. L. *Org. Biomol. Chem.* **2008**, *6*, 2204–2212.

(47) Koder, R. L., Jr.; Lichtenstein, B. R.; Cerda, J. F.; Miller, A.-F.; Dutton, P. L. *Tetrahedron Lett.* **2007**, *48*, 5517–5520.

(48) Tamura, N.; Mitsui, K.; Nabeshima, T.; Yano, Y. *J. Chem. Soc., Perkin Trans.* **1994**, *2*, 2229–2237.

(49) Bennett, A. E.; Rienstra, C. M.; Auger, M.; Lakshmi, K. V.; Griffin, R. G. *J. Chem. Phys.* **1995**, *103*, 6951–6958.

(50) Mason, J. In *Encyclopedia of NMR*; Grant, D. M., Harris, R. K., Eds.; Wiley: Sussex UK, 1996; pp 3222−3251.

(51) Herzfeld, J.; Berger, R. *J. Chem. Phys.* **1980**, *73*, 6021–6032.

(52) Eichele, K.; Wasylishen, R. E. HBA ver. 1.6, a program for performing Herzfeld−Berger Analysis; 2010, http://anorganik.uni-tuebingen.de/klaus/soft/index.php?p=hba/hba.

(53) Frisch, M. J. et al. *Gaussian 03*; Gaussian, Inc.: Wallingford, CT, 2004. The full reference is given in the Supporting Information.

(54) Müller, F.; Massey, V. *J. Biol. Chem.* **1969**, *244*, 4007–4016.

(55) Stephens, P. J.; Devlin, F. J.; Chabalowski, C. F.; Frisch, M. J. *J. Phys. Chem.* **1994**, *98*, 11623–11627.

(56) Becke, A. D. *J. Chem. Phys.* **1993**, *98*, 5648–5652.

(57) Ditchfield, R. J. *J. Chem. Phys.* **1972**, *56*, 5688–5691.

(58) Tomasi, J.; Persico, M. *Chem. Rev.* **1994**, *94*, 2027–2094.

(59) Jameson, C. J.; Jameson, A. K.; Oppusunggu, D.; Wille, S.; Burrell, P. M.; Mason, J. *J. Chem. Phys.* **1981**, *74*, 81–88.

(60) Boys, S. F.; Bernardi, F. *Mol. Phys.* **1970**, *19*, 553–566.
(61) Burant, J. C.; Strain, M. C.; Scuseria, G. E.; Frisch, M. J. *Chem. Phys. Lett.* **1996**, *258*, 45–52.
(62) Counterpoise corrected complex energies could only be performed without SCRF.
(63) Reed, A. E.; Weinstock, R. B.; Weinhold, F. *J. Chem. Phys.* **1985**, *83*, 735–746.
(64) Moonen, C. T. W.; Vervoort, J.; Müller, F. *Biochemistry* **1984**, *23*, 4859–4867.
(65) Stacking interactions can occur between flavins; however, we anticipate that the great excess of benzene will outcompete flavin stacking.
(66) The isotropic average from the SSNMR of TPARF + DBAP was 347.5 ± 0.8 ppm vs 349.8 ppm for TPARF + DBAP in solution.
(67) A small excess of DBAP powder could be seen in suspension prior to freezing.
(68) The structure of the TPARF/DBAP complex has not been determined crystallographically, nor has that of TARF/DAP. However, the structure is validated by NMR spectroscopy and the fact that our geometry optimizations retain the proposed structure and yield calculated CSPVs that agree with experiment.
(69) Perdew, J. P.; Wang, Y. *Phys. Rev. B* **1992**, *45*, 13244–13249.
(70) This is in part a reflection of the extreme sensitivity of NMR shieldings to geometry and interactions with the environment.
(71) Hermann, C.; Ilich, P.; Hille, R. *J. Phys. Chem. B* **2003**, *107*, 2139–2156.
(72) Fersht, A. *Structure and Mechanism in Protein Science*; Freeman and Co.: New York, 1999.
(73) Girvan, H. m.; Marshall, K. R.; Lawson, R. J.; Leys, D.; Joyce, M. G.; Clarkson, J.; Smith, W. E.; Cheesman, M. R.; Munro, A. W. *J. Biol. Chem.* **2004**, *279*, 23274–23286.
(74) Pavel, E. G.; Zhou, J.; Busby, R. W.; Gunsior, M.; Townsend, C. A.; Solomon, E. I. *J. Am. Chem. Soc.* **1998**, *120*, 743–753.
(75) Palfey, B. A.; Moran, G. R.; Entsch, B.; Ballou, D. P.; Massey, V. *Biochemistry* **1999**, *38*, 1153–1158.
(76) Stueber, D.; Grant, D. M. *J. Am. Chem. Soc.* **2002**, *124*, 10539–10551.
(77) Schramek, N.; Haase, I.; Fischer, M.; Bacher, A. *J. Am. Chem. Soc.* **2003**, *125*, 4460–4466.
(78) Kim, R.-R.; Illarionov, B.; Joshi, M.; Cushman, M.; Lee, C. Y.; Eisenreich, W.; Fischer, M.; Bacher, A. *J. Am. Chem. Soc.* **2010**, *132*, 2983–2990.
(79) Sedlmaier, H.; Müller, F.; Keller, P. J.; Bacher, A. *Z. Naturforsch.* **1987**, *42*, 425–429.
(80) Niemz, A.; Rotello, V. *J. Mol. Recognit.* **1996**, *9*, 158–162.
(81) Mayhew, S. G. *Eur. J. Biochem.* **1999**, *265*, 698–702.
(82) Curley, G. P.; Carr, M. C.; Mayhew, S. G.; Voordouw, G. *Eur. J. Biochem.* **1991**, *202*, 1091–1100.
(83) Our calculations nonetheless suggest that we would not expect much larger effects even if the TPARF were not subject to dimerization in solution.
(84) Facelli, J. C.; Pugmire, R. J.; Grant, D. M. *J. Am. Chem. Soc.* **1996**, *118*, 5488–5489.